Proceedings of the ASME 2019 International Design Engineering Technical Conferences & Computers and Information in Engineering Conference
IDETC/CIE 2019
August 18-21, 2019, Anaheim, CA, USA

IDETC2019-98389

DESIGN OF FOUR-, SIX-, AND EIGHT-BAR LINKAGES FOR RECTILINEAR MOVEMENT

Xueao Liu*
School of Mechanical Engineering and Automation, Beihang University
Beijing, 100083, China
Robotics and Automation Laboratory
University of California
Irvine, California 92697
Email: liuxueao@buaa.edu.cn

Jeffrey Glabe
Robotics and Automation Laboratory
University of California
Irvine, California 92697
Email: jglabe@uci.edu

Hongyu Wu
School of Mechanical Engineering
Tsinghua University
Beijing, 100084, China
Email: wu-hy18@mails.tsinghua.edu.cn

Chunjie Wang
School of Mechanical Engineering and Automation, Beihang University
Beijing, 100083, China
Email: wangcj@buaa.edu.cn

J. Michael McCarthy
Robotics and Automation Laboratory
University of California
Irvine, California 92697
Email: jmmccart@uci.edu

ABSTRACT

This paper examines the results of synthesis algorithms for four-, six-, and eight-bar linkages for rectilinear movement. Rectilinear movement is useful for applications such as suspensions that provide linear movement with out a rotation component. The algorithm yields one four-bar, seven six-bar, and 32 eight-bar linkages. The synthesis strategy begins with a task guided by a multi-degree of freedom chain. The algorithm computes constraints to guide the required movement with one degree-of-freedom. Each computed design is analyzed to ensure smooth movement through the specified set of task positions. Finally, we identify the design that has the least variation from a pure rectilinear movement.

*Address all correspondence to this author.

INTRODUCTION

This presents a design study of kinematic synthesis of linkages that provide rectilinear movement. We present a synthesis strategy for four-bar, six-bar and eight-bar linkages and compare the performance of the resulting designs.

The main synthesis theory are RR constraints and inverse kinematics of 3R chain. According to Burmester's theory, an RR constraint link can through exactly five task configurations at most. On this paper, we specify five task points which are in a straight line. Notice that any five points can be specified by designer.

For four-bar linkage, we specify a set of five task positions and calculate the two RR constraints that guide the movement, and obtain six four-bar linkage candidates at most. Our synthesis method of six-bar is adding two RR constraints to the inverse kinematics solution of a RRR chain, and we obtain seven six-bar linkages and a maximum of 75 linkage candidates. Then we solve two inverse kinematics of a RRR chain to get a 6R chain,

Copyright © 2019 by ASME

and add two RR constraints to maintain the relative positions of the links, so a eight-bar linkage is constructed. We obtain 32 eight-bar linkages and 340 candidates.

For synthesized linkages, we use the Dixon determinant theory to solve it. The results of Dixon determinant are simple to derive and implement, in addition, it can figure out all of the linkage configuration when the input angle at each value in rotated of the input range.

For the a given value of the input angle, we can obtain more than one set of solutions using the Dixon determinant. When the input link rotates sequentially in the range, it will generate more than one branch. There are 2 branches at most for six-bar linkages, 6 branches for six-bar linkages and 18 branches for eight-bar linkages. We use Newton's iteration to sort these branches, and check whether the five task positions are on one of these sorted branches or not. If yes, we can obtain a non-defect linkage to through the task positions in a smooth movement.

At last, we give an example of configuration the five task positions that on a straight line. And we obtain a series of non-defect four-bar, six-bar and eight-bar linkages. From the comparison, we find that the eight-bar linkage is the most accurate to the rectilinear motion.

LITERATURE SURVERY

The design of linkage systems to generate rectilinear movement can be traced back to a paper in 1875 by A. B. Kempe [1], also see Kempe [2]. The use of rectilinear linkages in suspension systems have the advantage of maintaining design parameters during suspension deformation, see Zhao et al. [3, 4]. Yang and McCarthy [5] examined the design of compliant eight-bar linkages for use as suspensions of MEMs gyroscopes. Weeke et al. [6] show the use of rectilinear movement in force balanced oscillators, and Hopkins and Gupta [7] demonstrate the use of rectilinear movement in snake robots.

Our strategy for the design of RR constraints to guide a body through a set of task positions was introduce by L. Burmester [8], also see McCarthy and Soh [9]. Soh and McCarthy [10] added two RR constraints to a RRR serial chains to design six-bar linkages, then using the same idea they added two RR constraints to a 6R closed chain to design eight-bar linkages [11].

An important part of the design process is performance verification, and the generation of new designs. Each linkage is analyzed using the method of Dixon determinants described by Wampler [12], in order to ensure that it moves smoothly through the task positions. Our formulation is based on the automated generation of the loop equations developed by Parish and McCarthy [13]. The task positions are modified within user defined tolerances to generate more designs, as presented by Plecnik and McCarthy [14, 15].

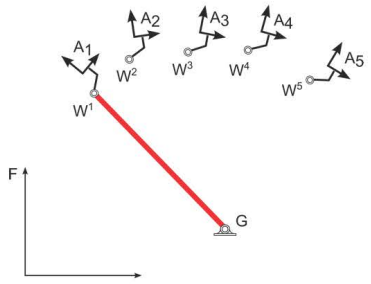

FIGURE 1. A PIVOT **G** AND A MOVING PIVOT **W** THAT TAKES THE SERIES OF POSITIONS $\mathbf{W}^i$ OF RR CONSTRAINT .

FOUR-BAR LINKAGE SYNTHESIS

Our synthesis strategy for a four-bar linkage is to specify a set of five task positions and compute the two RR constraints that guide the movement.

Figure 1, shows a pivot **G** and a moving pivot **W** that takes the series of positions $\mathbf{W}^i$,

$$\mathbf{W}^i = [A_i]\mathbf{w}, \quad i = 1, \ldots, 5, \tag{1}$$

where the matrices $[A_i]$ are the 3×3 homogeneous transforms that define five rectilinear positions of the moving body.

The synthesis equations are obtained from the constraint that the length of the link **GW** is constant,

$$([A_i][A_1]^{-1}\mathbf{W}^1 - \mathbf{G}).([A_i][A_1]^{-1}\mathbf{W}^1 - \mathbf{G}) = R^2, \quad i = 1, \ldots, 5 \tag{2}$$

We can get solve these equations to obtain four sets solutions for the link **GW**, which can be combined to yield as many as six four-bar candidates linkages.

Performance Verification for Four-bar Linkage

Each design for the four-bar linkage is analyzed by formulating its loop equations,

$$\begin{aligned} a_1 \cos\theta_1 + a_2 \cos\theta_2 + a_3 \cos\theta_3 + a_4 \cos\theta_4 = 0, \\ a_1 \sin\theta_1 + a_2 \sin\theta_2 + a_3 \sin\theta_3 + a_4 \sin\theta_4 = 0. \end{aligned} \tag{3}$$

Where $a_i, i = 1, \ldots, 4$ are the length of per link of the four-bar linkage, and $\theta_i, i = 1, \ldots, 4$ are the corresponding angles from the x axis of ground frame.

We solve these equations for the rotation of the input crank to verify the smooth movement of the linkage through the task positions. If the linkage jams or cannot reach a task position is it removed.

In order to obtain useful linkages, we modify the task within user specified tolerances, and generate new design candidates. A

Copyright © 2019 by ASME

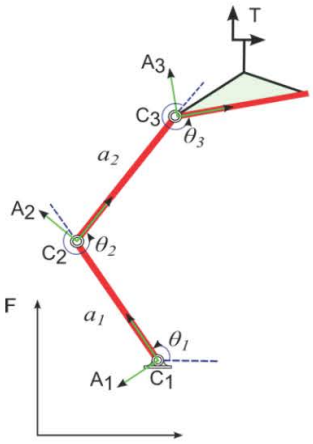

FIGURE 2. THE NOTATION OF THE INVERSE KINEMATICS OF A RRR CHAIN.

detailed description of this process is presented for an example of a six-bar below.

SIX-BAR LINKAGE SYNTHESIS

To design the six-bar linkage, we select an RRR serial chain that moves its end-effector through the required set of rectilinear task positions, Figure 2. The inverse kinematics solution for this chain defines the positions of each of its link in each configuration. From that information, we can compute two RR constraints that maintain the required relative positions of the links. The result is a six-bar linkage.

There are several ways that these two RR constraints can be added to the RRR serial chain, see Fig. 3(a). in a graph where the vertices represent links and the edges are joints, we obtain $\binom{4}{2=6}$ combinations of constraints. The adjacent links should be removed, so we obtain 3 types of RR constraint links, See Figure 3.

Inverse Kinematics of RRR chain

As shown in figure 2, T is the task position, and the displacement transformation matrix of $[T]$ is $[K(\theta_1,\theta_2,\theta_3)]$ in the ground frame F. Let $[G]$ represents the transformation matrix of base in ground frame F, and $[H]$ represents the transformation matrix of end effector in frame A_3 . The position of each link frames can be denoted by $A_i, i=1,2,3$. So the kinematics equations of RRR chain can be expressed by

$$[K(\theta_1,\theta_2,\theta_3)] = [G].[A_1(\theta_1)].[A_2(\theta_2,a_1)].[A_2(\theta_3,a_2)].[H] \quad (4)$$

where $[\theta_1,\theta_2,\theta_3]$ are the joint relative rotation angles of the RRR chain, and we can get the values by solving this matrix equation.

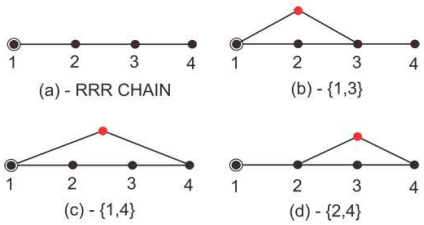

FIGURE 3. RRR CHAIN GRAPH AND THE THREE CASES OF ADDING RR CONSTRAINT LINK.

For the five task positions $T_i, i=1,...,5$, we can use the equation (4) to solve the angles $\theta_{1i},\theta_{2i},\theta_{3i}$, which can be written as,

$$[T_i] = [K(\theta_{1i},\theta_{2i},\theta_{3i})] \quad (5)$$

Notice that these angles $\theta_{1i},\theta_{2i},\theta_{3i}$ are relative angles, we obtain the link transformation matrix A_{1i}, A_{2i}, A_{3i} relative to the ground frame F as,

$$\begin{aligned}
[A_{1i}] &= [G].[A_1(\theta_{1i})],\\
[A_{2i}] &= [G].[A_1(\theta_{1i})].[A_2(\theta_{2i},a_1)], \qquad i=1,\ldots,5. \quad (6)\\
[A_{3i}] &= [G].[A_1(\theta_{1i})].[A_2(\theta_{2i},a_1)].[A_2(\theta_{3i},a_2)],
\end{aligned}$$

Add Two RR Constraints

There are four ways to add two RR constraint to the four links that form the RRR chain, see Figure 4.

When one RR constraint is designed, we obtain a fifth link that can be used to constrain the linkage. There are three cases to consider, RR constraint that connects links $\{\{1,3\},\{1,4\}$, and $\{2,4\}\}$. In each case, an RR chain can be connected between the new link 5 and any of the remaining bodies.

For the case that $\{1,3\}$, we can design the second RR constraint as $\{5,2\}$ or $\{5,4\}$, see Fig. 5. Notice that the combination of constraints $\{1,3\}$-$\{5,2\}$ yields a structure, so this case is eliminated. For the case of $\{1,4\}$, we can design the second RR constraint as $\{5,2\}$ and $\{5,3\}$, see Fig. 6. For the case of $\{2,4\}$, we design the RR constraints $\{5,1\}$ and $\{5,3\}$. The linkage $\{2,4\}$-$\{5,1\}$ is the same as the case of $\{1,3\}$- $\{2,4\}$. Finally, $\{2,4\}$-$\{5,3\}$ is shown as Fig. 7, which must be eliminated because the four-bar sub-loop structure rotates freely as a whole around link 1.

The result is that we obtain a total of seven six-bar linkages by adding two RR constraints. There are as many as 4 sets solutions of RR constraint, so we can obtain a maximum of $5\times(3\times4)+3\times3+6=75$ of six-bar linkage candidates.

Copyright © 2019 by ASME

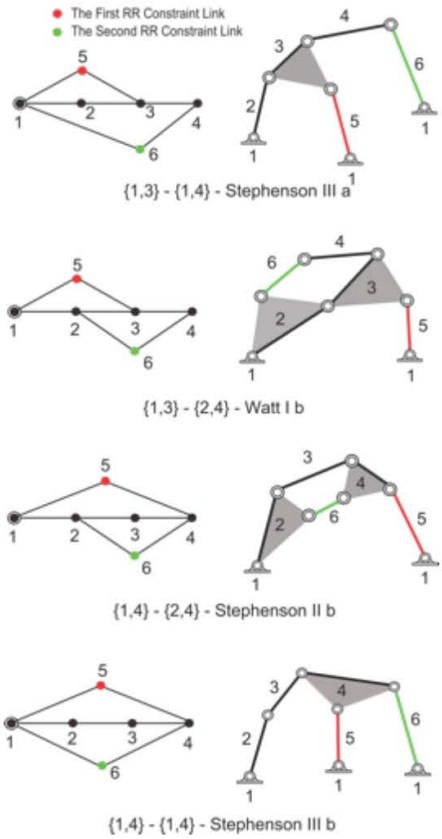

FIGURE 4. FOUR WAYS TO ADD RR CONSTRAINT TO THE FOUR LINKS THAT FORM THE RRR CHAIN.

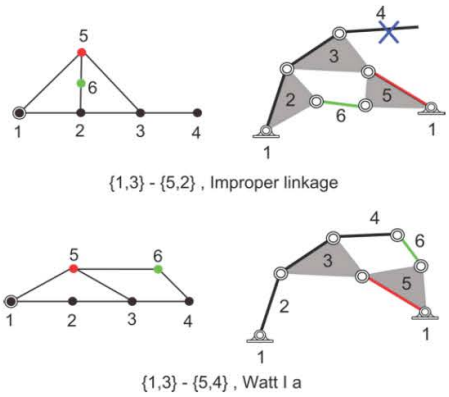

FIGURE 5. THE CASE OF $\{1,3\}$ AS THE FIFTH LINK, WE CAN DESIGN THE SECOND RR CONSTRAINTS AS $\{5, 2\}$ or $\{5, 4\}$, AND THE CASE OF $\{1, 3\}$-$\{5, 2\}$ YIELDS A STRUCTURE WHICH SHOULD BE ELIMINATED .

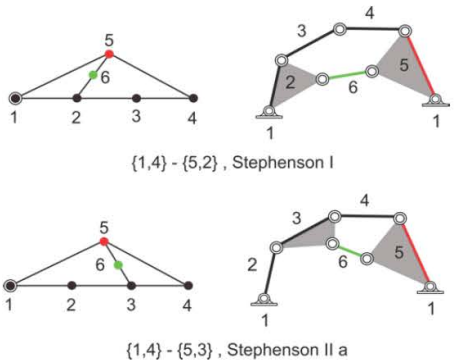

FIGURE 6. THE CASE OF $\{1,4\}$ AS THE FIFTH LINK, WE CAN DESIGN THE SECOND RR CONSTRAINTS AS $\{5, 2\}$ OR $\{5, 3\}$.

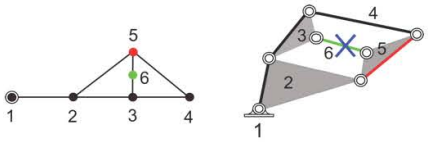

FIGURE 7. THE CASE OF $\{2,4\}$ AS THE FIFTH LINK, THE $\{5, 2\}$, $\{5, 3\}$ CONSTRAINTS GENERATE THE FOUR-BAR SUB-LOOP STRUCTURE AND SHOULD BE ELIMINATED.

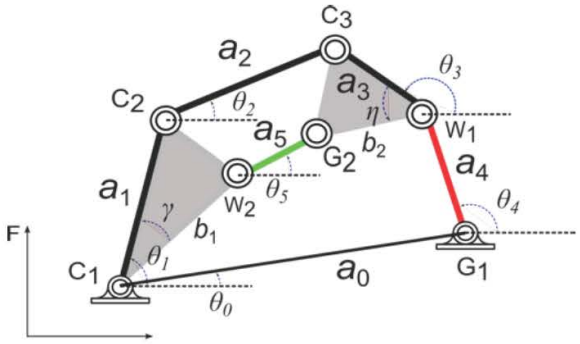

FIGURE 8. THE NOTATION OF STEPHENSON II B AS AN EXAMPLE OF SOLVING FORWARD KINEMATICS FOR PERFORMANCE VERIFICATION.

Performance Verification for Six-Bar Linkage

Each design for the six-bar linkage is analyzed by formulating its loop equations, an example of Stephenson II b six-bar linkage is demonstrated, the notation of it is shown as Fig. 8.

A six-bar linkage has two independent loops, for Stephenson II b, there are $C_1 - C_2 - C_3 - W_1 - G_1$ and $C_1 - W_2 - G_2 - W_1 - G_1$. We can easily obtain the kinematics equation of Stephenson

Copyright © 2019 by ASME

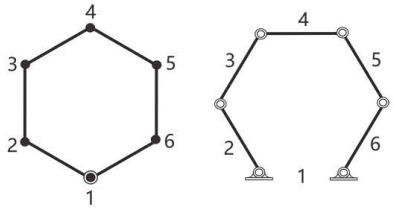

FIGURE 9. THE 6R CHAIN AND IT'S GRAPH WHICH IS COMPRISED OF TWO RRR SERIES CHAINS.

II b which given by

$$
\begin{aligned}
f_1 &: a_1\cos\theta_1 + a_2\cos\theta_2 - a_3\cos\theta_3 - a_4\cos\theta_4 - a_0\cos\theta_0 = 0,\\
f_2 &: a_1\sin\theta_1 + a_2\sin\theta_2 - a_3\sin\theta_3 - a_4\sin\theta_4 - a_0\sin\theta_0 = 0,\\
f_3 &: b_1\cos(\theta_1-\gamma) + a_5\cos\theta_5 - b_2\cos(\theta_3+\eta) - a_4\cos\theta_4 = 0,\\
f_4 &: b_1\sin(\theta_1-\gamma) + a_5\sin\theta_5 - b_2\sin(\theta_3+\eta) - a_4\sin\theta_4 = 0.
\end{aligned}
\tag{7}
$$

Where θ_0, γ and η are constants, θ_1 is input angle, the variables are $\theta_j, j = 2,\ldots,5$.

We solve these equations for the rotation of the input crank to verify the smooth movement of the linkage through the task positions. In order to obtain useful linkages, we also modify the task within user specified tolerances, and generate more new design candidates. A detailed description of solving this process is presented later.

EIGHT-BAR LINKAGE SYNTHESIS

To design the eight-bar linkage, we construct a 6R chain which is comprised of two RRR series chains, Fig. 9. Then we compute two RR constraints that keep the 6R chain through the task positions with one degree of freedom. The result is a eight-bar linkage.

For the 6R chain graph, we can obtain $\binom{6}{2=15}$ combinations of constraints. Notice that this paper only focus on the case of two joints on the ground link of eight-bar linkages. Remove the adjacent links and the types of RR constraint links which connect on ground link, then we obtain 6 feasible combinations of constraints, see Fig. 10.

Add Two RR Constraints For 6R Chain.

There are 17 ways to add two RR constraints to the 6R chain to obtain a eight-bar linkage, see Fig. 11.

When one RR constraint is designed, we obtain a seventh link that can be used to constrain the linkage. And there are six cases to consider, RR constraint that connects links $\{\{2, 4\}, \{2, 5\}, \{2, 6\}, \{3, 5\}, \{3, 6\}$, and $\{4, 6\}\}$. In each case, an RR

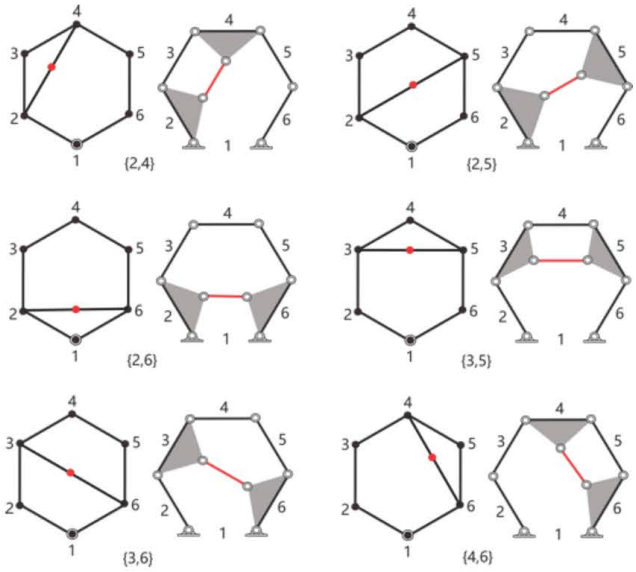

FIGURE 10. SIX CASES OF EIGHT-BAR LINKAGE WITH ADDING ONE RR CONSTRAINT LINK

constraint can be connected between the new link 7 and any of the remaining bodies except ground link.

For the case of $\{2, 4\}$, we can obtain $\{\{2, 4\}$-$\{7, 1\}\}$, $\{\{2, 4\}$-$\{7, 3\}\}$, $\{\{2, 4\}$- $\{7, 5\}\}$ and $\{\{2, 4\}$- $\{7, 6\}\}$ which are shown as Fig. 12. Notice that the combination of constraints $\{\{2, 4\}$- $\{7, 1\}\}$ yields the third joint connect to the ground link, and the combination of constraints $\{\{2, 4\}$- $\{7, 3\}\}$ generates the four-bar sub-loop structure, so these two case are eliminated. And so on, we obtain 15 combinations of constraints using this method, see Fig. 13.

The result is that we obtain a total of thirty-two eight-bar linkages by adding two RR constraints. And we also can obtain $178 + 162 = 340$ eight-bar linkage candidates.

Performance Verification for Eight-Bar Linkage

Each design for the eight-bar linkage is analyzed by formulating its loop equations, an example of an eight-bar linkage $\{\{2,4\}$-$\{2,5\}\}$ is demonstrated, the notation of it is shown as Fig. 14.

An eight-bar linkage has three independent loops, for this one, there are $C_1 - C_9 - C_{10} - C_5 - C_6$, $C_1 - C_7 - C_8 - C_4 - C_5 - C_6$ and $C_1 - C_2 - C_3 - C_4 - C_5 - C_6$. We obtain the loop equations, see Eqn. 8.

We solve these equations for the rotation of the input crank to verify the smooth movement of the linkage through the task positions. In order to obtain useful linkages, we also modify the task within user specified tolerances, and generate more new design candidates. The process of solving the loop equation and

Copyright © 2019 by ASME

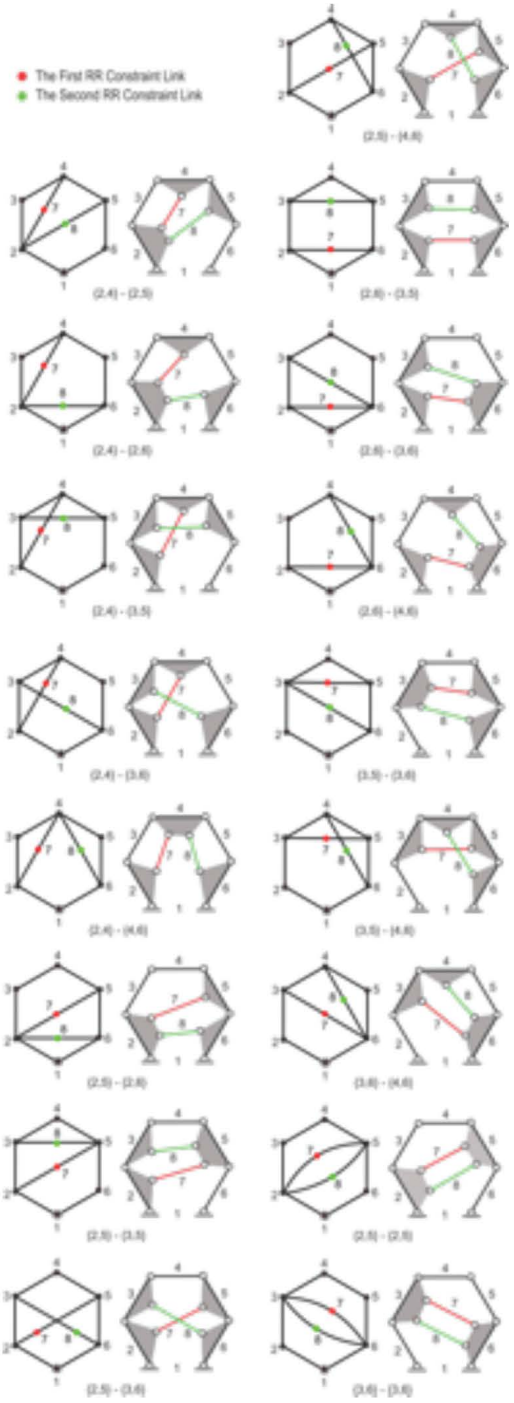

FIGURE 11. 17 WAYS TO ADD TWO RR CONSTRAINTS TO A 6R CHAIN TO OBTAIN A EIGHT-BAR LINKAGE.

verifying the performance are demonstrated by an example of the Stephenson II b linkage.

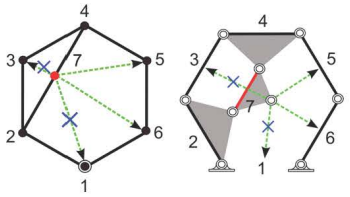

FIGURE 12. {2,4} AS THE SEVENTH LINK, THE CASE OF {{2, 4}-{7, 1}} YIELDS THE THIRD JOINT CONNECT TO THE GROUND LINK, AND THE CASE OF {{2, 4}-{7, 3}} GENERATES THE FOUR-BAR SUB-LOOP STRUCTURE, THESE TWO CASES NEED BE ELIMINATED.

$$
\begin{aligned}
b_1\cos(\theta_1-\gamma_1-\gamma_2)+a_8\cos\theta_8-b_3\cos(\theta_4+\eta_1)\\
-a_5\cos\theta_5-a_6\cos\theta_6=0\\
b_1\sin(\theta_1-\gamma_1-\gamma_2)+a_8\sin\theta_8-b_3\sin(\theta_4+\eta_1)\\
-a_5\sin\theta_5-a_6\sin\theta_6=0\\
b_2\cos(\theta_1-\gamma_2)+a_7\cos\theta_7+b_4\cos(\theta_3+\eta_2)\\
-a_4\cos\theta_4-a_5\cos\theta_5-a_6\cos\theta_6=0\\
b_2\sin(\theta_1-\gamma_2)+a_7\sin\theta_7+b_4\sin(\theta_3+\eta_2)\\
-a_4\sin\theta_4-a_5\sin\theta_5-a_6\sin\theta_6=0\\
-a_1\cos\theta_1+a_2\cos\theta_2+a_3\cos\theta_3-a_4\cos\theta_4\\
-a_5\cos\theta_5-a_6\cos\theta_6=0\\
-a_1\sin\theta_1+a_2\sin\theta_2+a_3\sin\theta_3-a_4\sin\theta_4\\
-a_5\sin\theta_5-a_6\sin\theta_6=0
\end{aligned}
\tag{8}
$$

Where θ_6, γ_1, γ_2, η_1 and η_2 are constants. And θ_1 is input angle, the variables of input angle are $\theta_i, i=2,3,4,5,7,8$.

AN EXAMPLE OF PERFORMANCE VERIFICATION

In this section, we use the Stephenson II b six-bar linkage as an example to demonstrate the process of performance verification.

Kinematics Equations For Dixon Determinant

We use the Dixon Determinant to solve the loop equations of all linkages. For Stephenson II b six-bar linkage, the kinematics loop equation is shown in Eqn. 7, now introduce the complex numbers $\Theta_j=e^{i\theta_j}$, where $i^2=-1$, so the kinematics equation (7) can be written by the complex form, that is

$$
\begin{aligned}
F_1 &: a_1\Theta_1+a_2\Theta_2-a_3\Theta_3-a_4\Theta_4-a_0e^{i\theta_0}=0,\\
F_2 &: a_1\Theta_1e^{-i\theta_\gamma}+a_5\Theta_5-b_2\Theta_3e^{i\theta_\eta}-a_4\Theta_4=0.
\end{aligned}
\tag{9}
$$

Copyright © 2019 by ASME

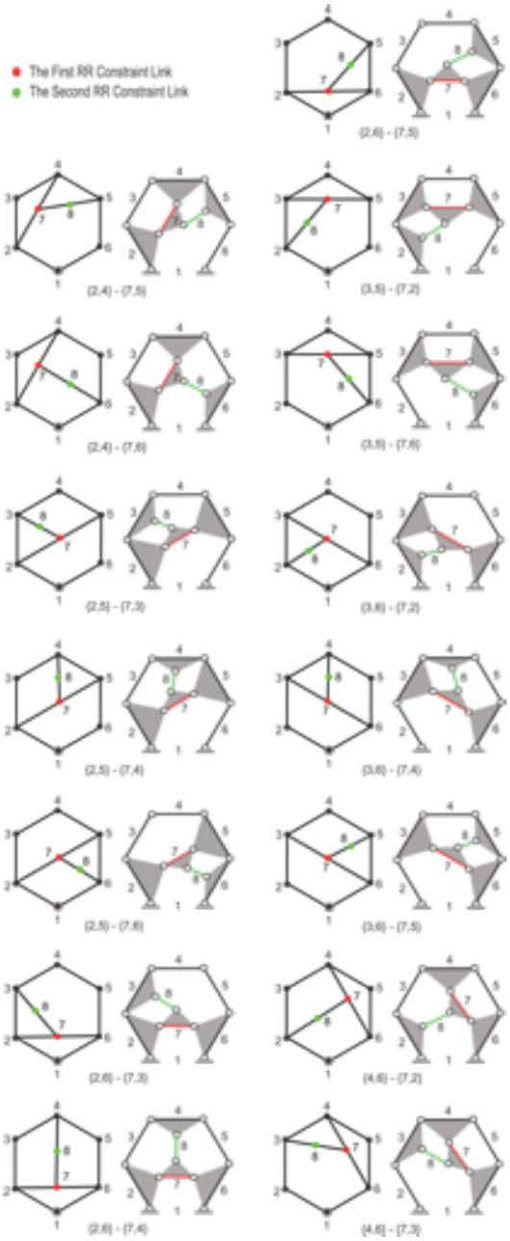

FIGURE 13. THE 15 EIGHT-BAR LINKAGES OF DEPENDENT SYNTHESIS METHOD.

The complex conjugate of Eqn. 9 can generate another two complex equations,

$$\begin{aligned} F_1^* &: a_1\Theta_1^{-1} + a_2\Theta_2^{-1} - a_3\Theta_3^{-1} - a_4\Theta_4^{-1} - a_0 e^{-i\theta_0} = 0, \\ F_2^* &: a_1\Theta_1^{-1} e^{i\theta_\gamma} + a_5\Theta_5^{-1} - b_2\Theta_3^{-1} e^{-i\theta_\eta} - a_4\Theta_4^{-1} = 0. \end{aligned} \tag{10}$$

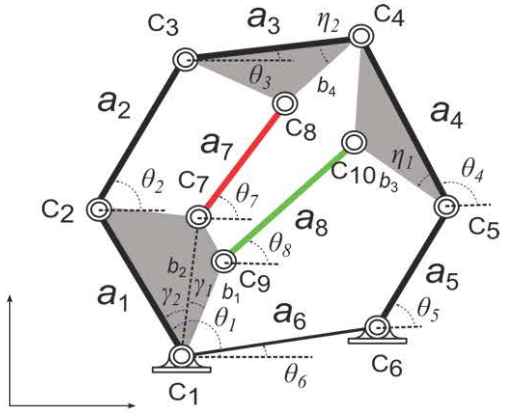

FIGURE 14. THE NOTATION OF AN EIGHT-BAR LINKAGE {{2,4}-{2,5}} OF SOLVING FORWARD KINEMATICS FOR PERFORMANCE VERIFICATION.

Forming the Dixon Determinant

The complex equations 9 and 10 determine four variables, $\Theta_j, j = 2,...5$, and Θ_1 is the input angle. Now we see Θ_2 as output angle and suppress it, so the four equations have three variables Θ_3, Θ_4 and Θ_5. Introduce $\alpha_j, j = 3,4,5$, we can get the Dixon determinant pattern as below,

$\Delta =$

$$\begin{vmatrix} F_1(\Theta_3,\Theta_4,\Theta_5) & F_1^*(\Theta_3,\Theta_4,\Theta_5) & F_2(\Theta_3,\Theta_4,\Theta_5) & F_2^*(\Theta_3,\Theta_4,\Theta_5) \\ F_1(\alpha_3,\Theta_4,\Theta_5) & F_1^*(\alpha_3,\Theta_4,\Theta_5) & F_2(\alpha_3,\Theta_4,\Theta_5) & F_2^*(\alpha_3,\Theta_4,\Theta_5) \\ F_1(\alpha_3,\alpha_4,\Theta_5) & F_1^*(\alpha_3,\alpha_4,\Theta_5) & F_2(\alpha_3,\alpha_4,\Theta_5) & F_2^*(\alpha_3,\alpha_4,\Theta_5) \\ F_1(\alpha_3,\alpha_4,\alpha_5) & F_1^*(\alpha_3,\alpha_4,\alpha_5) & F_2(\alpha_3,\alpha_4,\alpha_5) & F_2^*(\alpha_3,\alpha_4,\alpha_5) \end{vmatrix}. \tag{11}$$

Δ equates zero because each element of first row of Δ is zero, and the complex kinematics equations can be written as the general form, that is,

$$\begin{aligned} F_k &: c_{k0} + c_{k2}x + \sum_{j=3}^{5} c_{kj}\Theta_j, \\ & \qquad\qquad k = 1,2 \\ F_k^* &: c_{k0}^* + c_{k2}^* x^{-1} + \sum_{j=3}^{5} c_{kj}^*\Theta_j^{-1}, \end{aligned} \tag{12}$$

where x represents output Θ_2.

Then we simplify using that subtracting the second row from the first row, sequentially, the third row from second row and the fourth row from the third row. Then we obtain,

Copyright © 2019 by ASME

$$\Delta = \begin{vmatrix} c_{13}(\Theta_3-\alpha_3) & c^*_{13}(\Theta_3^{-1}-\alpha_3^{-1}) & c_{23}(\Theta_3-\alpha_3) & c^*_{23}(\Theta_3^{-1}-\alpha_3^{-1}) \\ c_{14}(\Theta_4-\alpha_4) & c^*_{14}(\Theta_4^{-1}-\alpha_4^{-1}) & c_{24}(\Theta_4-\alpha_4) & c^*_{24}(\Theta_4^{-1}-\alpha_4^{-1}) \\ c_{15}(\Theta_5-\alpha_5) & c^*_{15}(\Theta_5^{-1}-\alpha_5^{-1}) & c_{25}(\Theta_5-\alpha_5) & c^*_{25}(\Theta_5^{-1}-\alpha_5^{-1}) \\ F_1(\alpha_3,\alpha_4,\alpha_5) & F_1^*(\alpha_3,\alpha_4,\alpha_5) & F_2(\alpha_3,\alpha_4,\alpha_5) & F_2^*(\alpha_3,\alpha_4,\alpha_5) \end{vmatrix}. \tag{13}$$

Noticing $\Theta_j - \alpha_j = -\Theta_j\alpha_j(\Theta_j^{-1} - \alpha_j^{-1})$, plug it into equation (13), and rescale row j by factoring out $(\Theta_j^{-1} - \alpha_j^{-1})$, it can obtain the determinant δ which given by,

$$\delta = \begin{vmatrix} -c_{13}\Theta_3\alpha_3 & c^*_{13} & -c_{23}\Theta_3\alpha_3 & c^*_{23} \\ -c_{14}\Theta_4\alpha_4 & c^*_{14} & -c_{24}\Theta_4\alpha_4 & c^*_{24} \\ -c_{15}\Theta_5\alpha_5 & c^*_{15} & -c_{25}\Theta_5\alpha_5 & c^*_{25} \\ F_1(\alpha_3,\alpha_4,\alpha_5) & F_1^*(\alpha_3,\alpha_4,\alpha_5) & F_2(\alpha_3,\alpha_4,\alpha_5) & F_2^*(\alpha_3,\alpha_4,\alpha_5) \end{vmatrix}. \tag{14}$$

The result of determinant δ is a polynomial, It can be written as

$$\delta = \mathbf{a}^{\mathbf{T}}[W]\mathbf{t} = 0, \tag{15}$$

where $\mathbf{a}$, $\mathbf{t}$ are vectors of monomial, and $[W]$ is a 6×6 matrix, that are given by,

$$\mathbf{a} = \begin{pmatrix} \alpha_3 \\ \alpha_4 \\ \alpha_5 \\ \alpha_3\alpha_4 \\ \alpha_3\alpha_5 \\ \alpha_4\alpha_5 \end{pmatrix}, \quad \mathbf{t} = \begin{pmatrix} \Theta_3 \\ \Theta_4 \\ \Theta_5 \\ \Theta_3\Theta_4 \\ \Theta_3\Theta_5 \\ \Theta_4\Theta_5 \end{pmatrix} \tag{16}$$

and

$$[W] = \begin{bmatrix} D_1x + D_2 & A^T \\ A & -(D_1^* + D_2^*) \end{bmatrix}, \tag{17}$$

where D_1, D_2 are 3×3 diagonal matrices and A is a 3×3 matrix, it can be obtained by factoring out polynomial δ.

Solving for the Output Variables

The equation 17 is to hold for arbitrary values of $\alpha_j, j = 3,4,5$, so we have the matrix equation

$$[W]\mathbf{t} = 0. \tag{18}$$

The equation (18) can be derived as,

$$[W]\mathbf{t} = \left[\begin{pmatrix} D_1 & 0 \\ A & -D_2^* \end{pmatrix} x - \begin{pmatrix} -D_2 & -A^T \\ 0 & D_1^* \end{pmatrix} \right] \mathbf{t} = [Mx - N]\mathbf{t} = 0. \tag{19}$$

It can be converted into a standard generalized eigenvalue problem, that is ,

$$N\mathbf{t} = xM\mathbf{t}. \tag{20}$$

We can get the values of eigenvalue $x = \Theta_2$ and the corresponding eigenvector $\mathbf{t} = (\Theta_3, \Theta_4, \Theta_5, \Theta_3\Theta_4, \Theta_3\Theta_5, \Theta_4\Theta_5)^T$. Notice the eigenvector $\mathbf{t}$ may be defined up to a constant which call μ, we can get the values of Θ_3, Θ_4 and θ_5 by calculating the ratios,

$$\Theta_3 = \frac{t_4}{t_2} = \frac{\mu\Theta_3\Theta_4}{\mu\Theta 4}, \quad \Theta_4 = \frac{t_4}{t_1} = \frac{\mu\Theta_3\Theta_4}{\mu\Theta 3}, \quad \Theta_5 = \frac{t_5}{t_1} = \frac{\mu\Theta_3\Theta_5}{\mu\Theta 3}. \tag{21}$$

For above procedure, we can obtain the solution of complex angle $\Theta_j, j = 1,\ldots,5$, as $\Theta_j = e^{i\theta_j}$, we convert it into the real number pattern to generate $\theta_j, j = 1,\ldots,5$.

Sorting Branches

For a certain value of input angle, solving the equation 21, the maximum of solutions of the eigenvalue and corresponding eigenvector are 6 sets in theory. It means that for a series of the value of $\theta_{1,k}, k = 1,\ldots,n$ in the range of input angle, where n represents divisions number of the range, and k denotes the index of input angle, there are as many as 6 sets of solutions that correspond to 6 branches. It can be expressed as $\theta_{j,k,l}$, where $j = 2,\ldots,5$, which represents variables angle index, $k = 1,\ldots,n$, and $l = 1,\ldots 6$, which denotes the index of branches. For convenience later, that is written as the pattern,

$$[\theta_{1,k}|S_k] = \left[\begin{array}{c|cccc} \theta_{1,k} & \theta_{2,k,1} & \theta_{3,k,1} & \theta_{4,k,1} & \theta_{5,k,1} \\ \theta_{1,k} & \theta_{2,k,2} & \theta_{3,k,2} & \theta_{4,k,1} & \theta_{5,k,2} \\ \theta_{1,k} & \theta_{2,k,3} & \theta_{3,k,3} & \theta_{4,k,1} & \theta_{5,k,3} \\ \theta_{1,k} & \theta_{2,k,4} & \theta_{3,k,4} & \theta_{4,k,4} & \theta_{5,k,4} \\ \theta_{1,k} & \theta_{2,k,5} & \theta_{3,k,5} & \theta_{4,k,5} & \theta_{5,k,5} \\ \theta_{1,k} & \theta_{2,k,6} & \theta_{3,k,6} & \theta_{4,k,6} & \theta_{5,k,6} \end{array}\right], k = 1,\ldots,n \tag{22}$$

For four-bar and eight-bar linkages, the dimension of matrix $[W]$ are 2×2 and 18×18 respectively. So there are a maximum of 2 branches and 18 branches respectively for four-bar and eight-bar linkages.

Copyright © 2019 by ASME

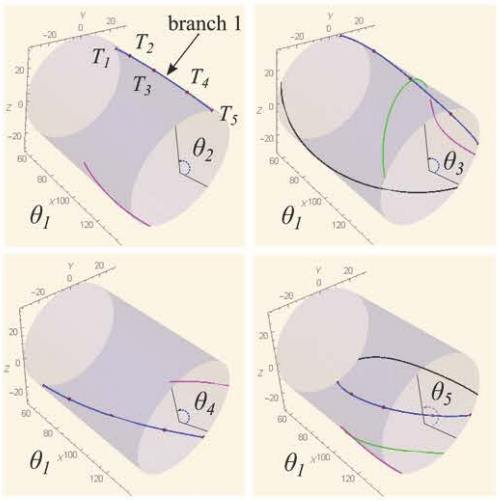

FIGURE 15. AN EXAMPLE OF FIVE TASK POINTS ON ONE BRANCH OF A SIX-BAR LINKAGE.

Here we also focus on the Stephenson II b, for the range of incremented input angle $\theta_{1,k}, k = 1,...,n$, the six branches are disordered from the range of θ_1 to θ_k. Here we use Newton's iteration method to sort them. It can be given by,

$$[S_{k+1}]_i = [S_k]_i - J_f^{-1}([S_k]_i) \cdot f([\theta_{1,k+1}], [S_k]_i), \quad k = 1,...,n-1, \quad \text{and} \quad i = 1,...,6, \tag{23}$$

where $f = [f_1, f_2, f_3, f_4]^T$ of the kinematics loop equations, and J_f is the Jacobian matrix of f, that is

$$[J_f] = \begin{bmatrix} -a_2 \sin\theta_2 & a_3 \sin\theta_3 & a_4 \sin\theta_4 & 0 \\ a_2 \cos\theta_2 & -a_3 \cos\theta_3 & -a_4 \cos\theta_4 & 0 \\ 0 & b_2 \sin(\theta_3 + \eta) & a_4 \sin\theta_4 & -a_5 \sin\theta_5 \\ 0 & -b_2 \cos(\theta_3 + \eta) & -a_4 \cos\theta_4 & a_5 \sin\theta_5 \end{bmatrix}. \tag{24}$$

Do several iteration of equation 24 can obtain the results of $[S_{k+1}]$ from $[S_k]$. So computing this equation and saving the results until $k = n-1$, the six branches can be generated and be sorted.

Checking Branches

When we get the sorted branches, we need to check the branches. Each branch represents a configuration of the linkage when input link rotates from θ_1 to θ_n. Now we check that whether the five task points are on one of these sorted branches or not. If there exist one branch satisfy it, this branch is the right branch, and this candidate linkage is a non-defect linkage. If not, this candidate linkage will be discarded. See an example as Fig. 15, the x axis is input angle θ_1 and the azimuth angle are $\theta_j, j = 2,\ldots,5$ respectively which are in the cylindrical coordinate frame. In this example, the five task points are on one of branches.

TABLE 1. THE FIVE TASK POSITION AND CORRESPONDING TOLERANCE.

Task	Orientation	Location(mm)	Tolerance $(\Delta\theta, \Delta x, \Delta y)$
1	0°	(0, 0)	(0°, 1.0, 1.0)
2	0°	(0, 25)	(5°, 1.0, 1.0)
3	0°	(0, 50)	(5°, 1.0, 1.0)
4	0°	(0, 75)	(5°, 1.0, 1.0)
5	0°	(0, 100)	(0°, 1.0, 1.0)

TABLE 2. THE RESULTS OF ITERATIONS OF FOUR-BAR LINKAGE.

No. of Iterations	No. of Candidates	No. of Non-Defect linkages
1	0	0
10	0	0
100	2	1

AN NUMERICAL EXAMPLE OF RECTILIEAR MOTION

In this section, we use the design algorithm to generate a rectilinear motion with four-bar, six-bar and eight-bar respectively. So the five task positions should be on a straight line. To obtain more candidate linkages, the tolerance zone $(\Delta\theta, \Delta x, \Delta y)$ for each task positions are constructed. The five task positions $T_i, i = 1,...,5$ and the corresponding tolerance that we used in this paper are shown in Table 1. Select randomly the sets of five task position in the specified tolerance zone, and do the iterations. Notice that doing the first iteration use the original five task position without tolerance. We do it by using Mathematica software.

Copyright © 2019 by ASME

TABLE 3. THE SOLUTIONS OF FOUR-BAR LINKAGE JOINTS.

Joint	Location
C_1	(-116.162, -49.643)
C_2	(-156.578,-102.258)
C_3	(88.0891,-155.43)
C_4	(128.261,-235.357)

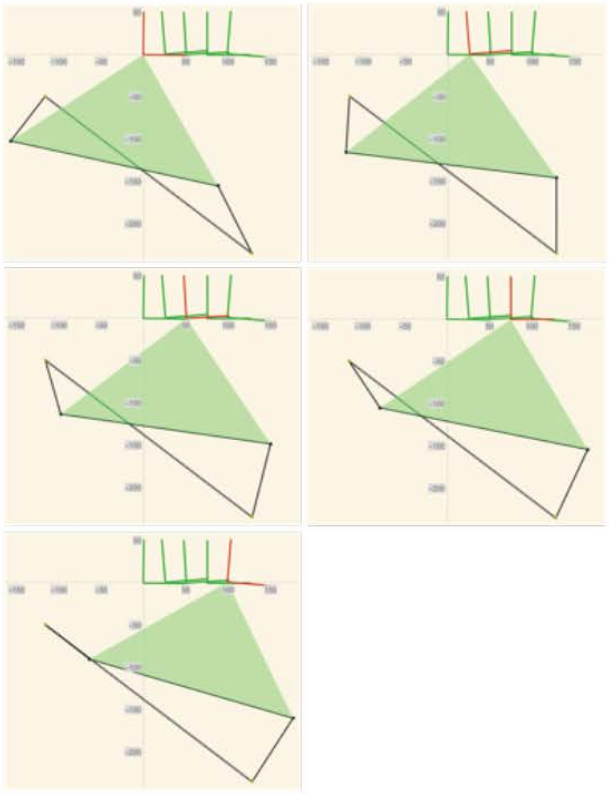

FIGURE 16. THE SELECTED FOUR-BAR LINKAGE THROUGH THE FIVE TASK POINTS OF RECTILINEAR MOVEMENT.

The Results of Four-Bar Linkage

For the four-bar linkage, we do 1 iteration, 10 iterations and 100 iterations. The results are in Table 2. As we can see, we only get one non-defect linkage from 100 iterations. From the results of 1 iteration, we can know there have no synthesized candidate linkage solution with original five task positions of the four-bar in this example. The solution of each joint location coordinate of the selected linkage is in Table 3, and the movement of the linkage through the five task positions are shown in Fig. 16. The

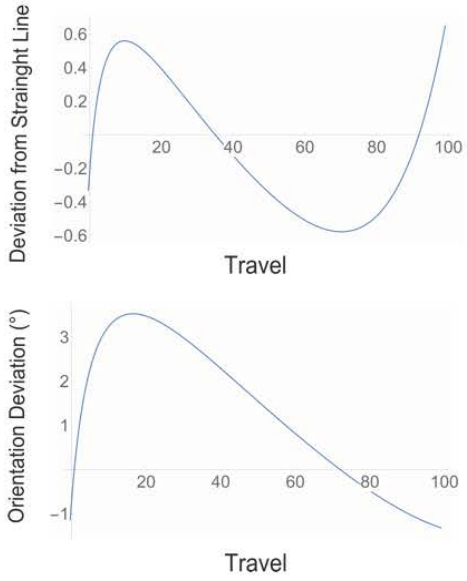

FIGURE 17. THE DEVIATION FROM STRAIGHT LINE AND ORIENTATION DEVIATION OF FOUR-BAR LINKAGE.

TABLE 4. THE JOINTS OF RRR CHAIN.

Joint	Location
C_1	(50.0, -140.0)
C_2	(100.0, -100.0)
C_3	(10.0, -30.0)

curves of deviation from straight line and the deviation of orientation for whole travel is in Fig. 17, the Maximum of deviation from straight line is 0.649425 mm and deviation of orientation is 3.52755° (61 milliradian).

The Results of Six-Bar Linkage

For the six-bar linkage, we need to specify the values of the base frame $[G]$, end effector frame $[H]$ and length of a_1 and a_2 of a RRR chain, these values are specified by designer. Here we give the Joints $C_i, i = 1,\ldots,3$ coordinate of the RRR chain in ground frame instead as shown in Table 4. The results of iteration are shown in Table 5. From the 1 iteration, we can know there have solutions of the original five task positions. For so many solutions, we use the minimum of sum of the deviation from straight line and the deviation of orientation to select the best one which moving trajectory is the most close to the rectilinear motion from these non-defect linkages. The result is one of Watt-I-a

Copyright © 2019 by ASME

TABLE 5. THE RESULTS OF ITERATIONS OF SIX-BAR LINKAGE.

No. of Iterations	No. of Candidates	No. of Non-Defect linkages
1	10	3
10	130	9
100	1270	68

TABLE 6. THE SOLUTIONS OF SIX-BAR LINKAGE JOINTS.

Joint	Location
C_1	(50.0,-140.0)
C_2	(100.0, -100.0)
C_3	(10.0, -30.0)
C_4	(95.6648,141.093)
C_5	(-9.52149,-246.415)
C_6	(-49.5215,-41.8701)
C_7	(-63.4494,-30.6536)

TABLE 7. THE JOINTS OF SIX-R CHAIN.

Joint	Location
C_1	(40.0, -150.0)
C_2	(100, -110)
C_3	(0.0, -10.0)
C_4	(30.0, -10.0)
C_5	(120, -90)
C_6	(0.0, -150.0)

linkage, and each joint location coordinate of the Watt-I-a linkage is in Table 6. And the movement of the linkage through the five task positions are shown in Fig. 18. The curves of deviation from straight line and the deviation of orientation for whole travel is in Fig. 19, the Maximum of deviation from straight line is 79 μm and deviation of orientation is 0.0368701° (643 μradian).

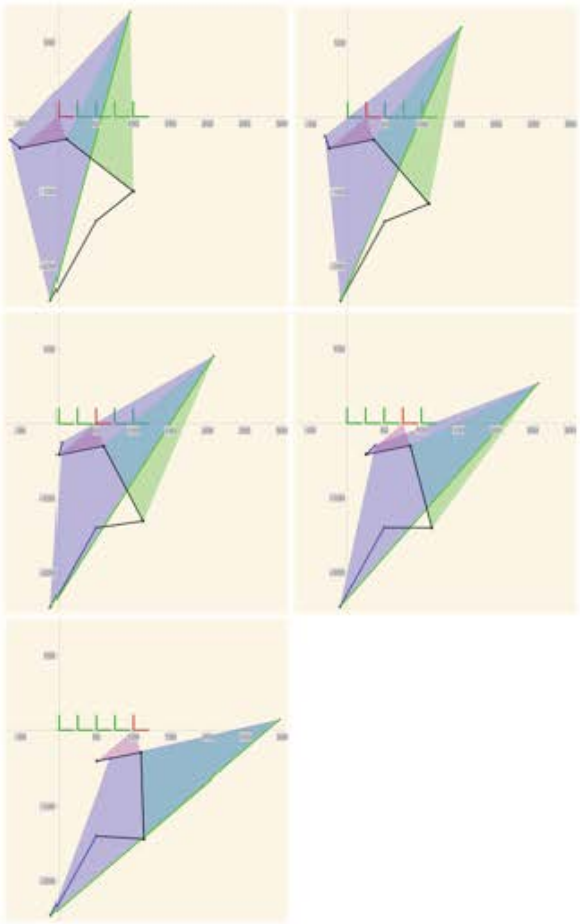

FIGURE 18. THE SELECTED SIX-BAR LINKAGE THROUGH THE FIVE TASK POINTS OF RECTILINEAR MOVEMENT.

The Results of Eight-Bar Linkage

For the eight-bar linkage, we specify the joints $C_i, i = 1, \ldots, 6$ coordinate of 6R chain in ground frame that is shown in Table 7. The results of iteration are shown in Table 8. From the 1 iteration, we can also know there are solutions of the original five task positions for eight-bar linkages. The best way we select is one of $\{\{2,5\}-\{4,6\}\}$ linkage which solutions are in Table 9. The movement of the linkage through the five task position are shown in Fig. 20. The curves of deviation from straight line and the deviation of orientation for whole travel is in Fig. 21, the Maximum of deviation from straight line is 5.7 μm and deviation of orientation is 0.0195578° (341 μradian).

Performance Comparison

From comparison of the solutions of four-bar, six-bar and eight-bar, we can know the largest number of non-defect linkages is eight-bar linkages, and the most accuracy of rectilinear motion

Copyright © 2019 by ASME

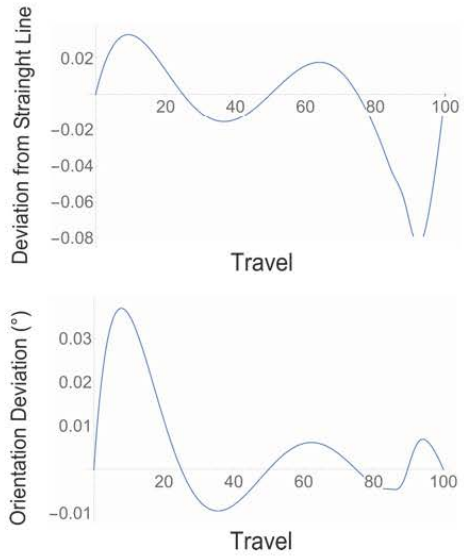

FIGURE 19. THE DEVIATION FROM STRAIGHT LINE AND ORIENTATION DEVIATION OF SIX-BAR LINKAGE.

TABLE 8. THE RESULTS OF ITERATIONS OF EIGHT-BAR LINKAGE.

No. of Iterations	No. of Candidates	No. of Non-Defect linkages
1	91	47
10	1179	114
100	11617	783

is also eight-bar linkages comparing with four-bar and six-bar linkages.

CONCLUSION

This paper studies the kinematic synthesis of four-bar, six-bar, and eight-bar linkages for a rectilinear movement task, and examines their relative performance. Rectilinear movement is useful for applications require linear movement with elimination associated rotational movement such as in micro suspension systems. These results show that our best four-bar linkage had a 0.65 mm deviation from the required straight line with an associated 61 milliradian variation in orientation. The six-bar linkage showed significant improvement in both measurements, with a 79 μm variation from a straight line with an associated 643 μradian variation in orientation. The eight-bar linkage performed even better with a 5.7 μm variation from a straight line and 341 μradian variation in orientation. This shows that a significant increase in performance can be achieved with the additional design opportunities available in an eight-bar linkage. In order to take advantage of this potential for a high level of precision further research in synthesis techniques that integrate the use of flexures for joints and link compliance are needed.

TABLE 9. THE SOLUTIONS OF EIGHT-BAR LINKAGE JOINTS.

Joint	Location
C_1	(40.0, -150.0)
C_2	(100, -110)
C_3	(0.0, -10.0)
C_4	(30.0, -10.0)
C_5	(120, -90)
C_6	(0.0, -150.0)
C_7	(135.618,-47.4867)
C_8	(123.256,-84.7386)
C_9	(-20.4555,52.8681)
C_{10}	(78.5251,-124.293)

ACKNOWLEDGMENT

Thanks to Prof. J. Michael McCarthy for helping me a lot for this paper. I also would like to thank Dr. Jeffrey Glabe to help me about the Mathematica software.

REFERENCES

[1] Kempe, A. B., 1875. "On a General Method of Producing Exact Rectilinear Motion by Linkwork". *Royal Society of London Proceedings,* ***23***, pp. 565–577.

[2] Kempe, A., 1877. *How to Draw a Straight Line: A Lecture on Linkages*. Cornell University Library historical math monographs. Macmillan and Company.

[3] Zhao, J.-S., Chu, F., and Feng, Z.-J., 2008. "Synthesis of Rectilinear Motion Generating Spatial Mechanism with Application to Automotive Suspension". *Journal of Mechanical Design,* ***130***(6), p. 065001.

[4] Zhao, J.-S., Liu, X., Feng, Z.-J., and Dai, J. S., 2012. "Stiffness of a rectilinear suspension with automatic length compensation branches". *Mechanism and Machine Theory*, pp. 99–122.

[5] Liu, Y., and McCarthy, J. M., 2015. "Flexure design for

Copyright © 2019 by ASME

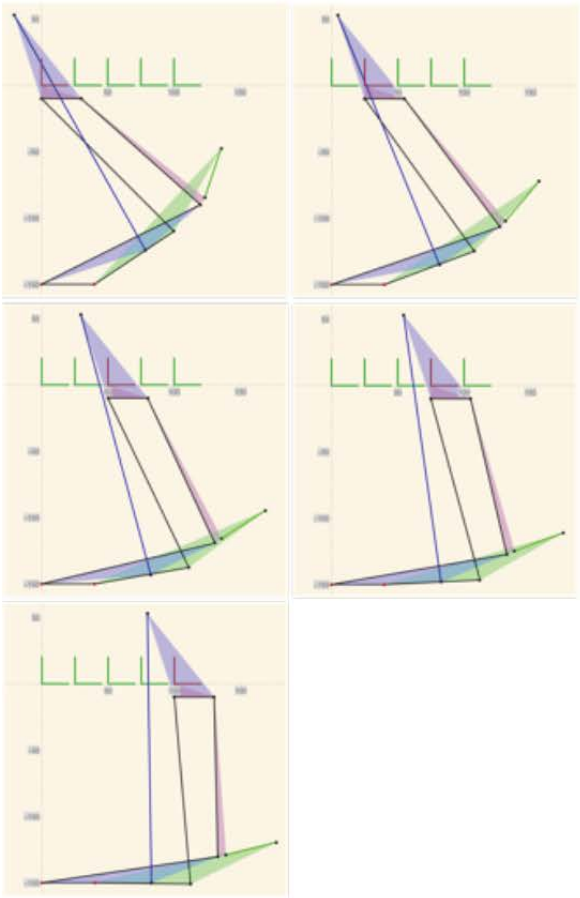

FIGURE 20. THE SELECTED EIGHT-BAR LINKAGE THROUGH THE FIVE TASK POINTS OF RECTILINEAR MOVEMENT.

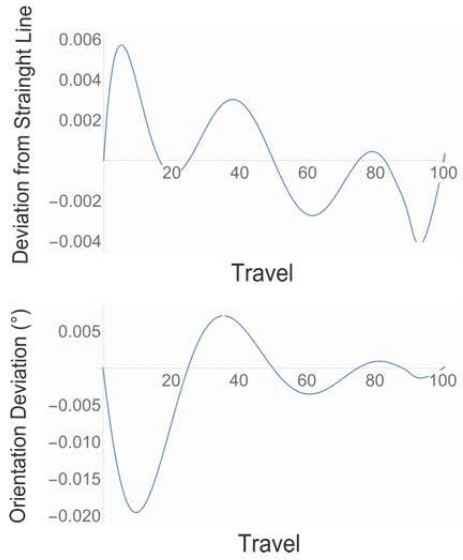

FIGURE 21. THE DEVIATION FROM STRAIGHT LINE AND ORIENTATION DEVIATION OF EIGHT-BAR LINKAGE.

eight-bar rectilinear motion mechanism". In Proceedings of the ASME 2015 International Design Engineering Technical Conferences and Computers and Information in Engineering Conference, ASME International.

[6] Weeke, S. L., Tolou, N., Semon, G., and Herder, J. L., 2017. "A monolithic force-balanced oscillator". *Journal of Mechanisms and Robotics,* ***9***.

[7] Hopkins, J. K., and Gupta, S. K., 2014. "Design and modeling of a new drive system and exaggerated rectilinear-gait for a snake-inspired robot". *Journal of Mechanisms and Robotics,* ***6***.

[8] Burmester, L. E. H., 1888. *Lehrbuch der Kinematik*. No. v. 1, pt. 1 in Lehrbuch der kinematik: Für studirende der machinentechnik, mathematik und physik geometrisch dargestellt. A. Felix.

[9] McCarthy, J. M., and Soh, G. S., 2011. *Geometric Design of Linkages*. Springer New York.

[10] Soh, G. S., and McCarthy, J. M., 2008. "The Synthesis of Six-Bar Linkages as Constrained Planar 3R Chains". *Mechanism and Machine Theory,* ***43***(2), pp. 160 – 170.

[11] Soh, G. S., and McCarthy, J. M., 2007. "Synthesis of Eight-Bar Linkages as Mechanically Constrained Parallel Robots". In Vol.653: 12th IFToMM world congress A.

[12] Wampler, C. W., 2001. "Solving the Kinematics of Planar Mechanisms by Dixon Determinant and a Complex-Plane Formulation". *Journal of Mechanical Design,* ***123***(3), p. 382.

[13] Parrish, B. E., and McCarthy, J. M., 2013. "Use of the Jacobian to Verify Smooth Movement in Watt I and Stephenson I Six-Bar Linkages". In Volume 6A: 37th Mechanisms and Robotics Conference, ASME.

[14] Plecnik, M. M., and McCarthy, J. M., 2012. "Design of a 5-SS Spatial Steering Linkage". In Volume 4: 36th Mechanisms and Robotics Conference, Parts A and B, ASME.

[15] Plecnik, M. M., and McCarthy, J. M., 2014. "Numerical Synthesis of Six-Bar Linkages for Mechanical Computation". *Journal of Mechanisms and Robotics,* ***6***(3), jun, p. 031012.

Copyright © 2019 by ASME